Article

Satellite Regional Cloud Climatology over the Great Lakes

Steven A. Ackerman [1,2,*], Andrew Heidinger [3], Michael J. Foster [1] and Brent Maddux [1,2]

[1] Cooperative Institute for Meteorological Satellite Studies, University of Wisconsin-Madison, Madison, WI 53706, USA; E-Mail: mfoster@aos.wisc.edu

[2] Department of Atmospheric and Oceanic Sciences, University of Wisconsin-Madison, Madison, WI 53706, USA; E-Mail: bcmaddux@wisc.edu

[3] Advanced Satellite Products Branch, NOAA, University of Wisconsin-Madison, Madison, WI 53706, USA; E-Mail: heidinger@ssec.wisc.edu

* Author to whom correspondence should be addressed; E-Mail: steva@ssec.wisc.edu; Tel.: +1-608-263-3647; Fax: +1-608-262-5974.

Abstract: Thirty-one years of imager data from polar orbiting satellites are composited to produce a satellite climate data set of cloud amount for the Great Lakes region. A trend analysis indicates a slight decreasing trend in cloud cover over the region during this time period. The trend is significant and largest (~2% per decade) over the water bodies. A strong seasonal cycle of cloud cover is observed over both land and water surfaces. Winter cloud amounts are greater over the water bodies than land due to heat and moisture flux into the atmosphere. Late spring through early autumn cloud amounts are lower over the water bodies than land due to stabilization of the boundary layer by relatively cooler lake waters. The influence of the lakes on cloud cover also extends beyond their shores, affecting cloud cover and properties far down wind. Cloud amount composited by wind direction demonstrate that the increasing cloud amounts downwind of the lakes is greatest during autumn and winter. Cold air flows over relatively warm lakes in autumn and winter generate wind parallel convective cloud bands. The cloud properties of these wind parallel cloud bands over the lakes during winter are presented.

1. Introduction

The Laurentian Great Lakes (Lake Superior, Lake Michigan, Lake Huron, Lake Erie and Lake Ontario) are a relatively recent geological feature, having formed from ice sheets 10,000 to 12,000 years ago. Collectively they form one of the largest reservoirs of fresh water in the world with a surface area of about 250,000 km^2 and holding about 22,800 km^3 of fresh water. The presence of these lakes, located near the center of the North American Continent, acts as a source of moisture that can have significant influence on the amount and distribution of cloudiness. Originally formed by melting glaciers, each year about 1% is water that originates from precipitation, rivers, and groundwater that drain into the lakes. The water level is a balance between those water sources and water loss due to evaporation and flow through the St. Lawrence River.

Given their geographic location and size, the lakes have a significant impact on the region's weather and climate. The 5 lakes span 7.5 degrees latitude, with the 45°N latitude line running through the center of the Great Lakes, which lay halfway between the equator and the North Pole. In the east–west direction they span about 800 m, between about 75°W and 95°W longitudes.

This investigation uses observations from satellite imaging systems to characterize the spatial cloud cover patterns over the Great Lakes region on time scales spanning daily influences to decadal trends. This study demonstrates how observed cloud patterns have changed over the ~30 year satellite time record. Changes in cloud cover and cloud properties associated with cold air outbreaks over the Great Lakes are also discussed.

2. Results and Discussion

2.1. AVHRR PATMOS-x

The Pathfinder Atmosphere Extended Project at NOAA, or PATMOS-x, aims to derive satellite data climate records from NOAA's satellite imager observations. The PATMOS-x data record includes the Advanced Very High Resolution Radiometer (AVHRR) imager flown on the NOAA Polar Orbiting Environmental Satellite Series (POES) since 1978 and more recently the European Organisation for the Exploitation of Meteorological Satellites' (EUMETSAT) Meteorological Operational (METOP) satellite series. This study uses PATMOS-x data from the AVHRR record that spans from 1981 to the present and provides global cloud products twice per day per satellite [1]. During most of the record, there were two satellites overpasses per day but more recently that number has increased to 3 or 4 overpasses. The 4-channel AVHRR record, with central wavelengths at 0.63, 0.86, 3.75 and 10.8 µm, begins in 1978 with the launch of TIROS-N; however, this study focusses on the 5-channel record (includes central wavelength at 12.0 µm), which began with the launch of NOAA-7. Processing is done using Global Area Coverage (GAC) data, for which each pixel is the mean of four 1.1 km AVHRR pixels, representing an area of approximately 3 km × 5 km. PATMOS-x employs ancillary data from the National Centers for Environmental Prediction Climate Forecast System Reanalysis (CFSR) [2]. The fields included in the PATMOS-x files are intended to facilitate the interpretation of the PATMOS-x products and to allow for further stratification of climate analyses. One of the key products of PATMOS-x is a probability of cloud determined by a Naïve Bayesian cloud detection scheme that uses multiple classifiers and surface types [3]. A pixel with a probability of

being cloud contaminated of greater than 0.5 is considered a cloudy pixel. The AVHRR PATMOS-x data set is sampled at a 0.1 degree equal-angle resolution on a fixed grid. The AVHRR PATMOS-x data is global but this analysis is limited to the region between 95°W and 75°W and 35°N and 55°N, therefore sampling issues that may arise from an equal-angle grid are not significant. The AVHRR PATMOS-x data is hosted at the NOAA National Climatic Data Center (NCDC).

Also included in the PATMOS-x analysis are the CFSR 10 m wind speed and direction data. The CFSR data have a spatial resolution of 0.5° and a temporal resolution of 6 hours. In this analysis, the CFSR data were temporally and spatially interpolated to match the PATMOS-x data.

2.2. Regional Overview

Figure 1 shows the 1982–2012 year average cloud amount over the region using the AVHRR observations and the PATMOS-x algorithm [3]. The mean shown in Figure 1 is computed from all of the AVHRR PATMOS-x data. No method to account for the variation in diurnal sampling time such as developed in [4] is applied. Figure 1 shows that the Great Lakes in general are more cloud covered than their surroundings though analysis shown later indicates that relative spatial distribution of cloud is a strong function of season and wind-direction. The mean cloud amount over the lakes is approximately 65%. In addition, there is a gradual gradient in cloudiness with lower values in the south and higher values north of the Lakes. Cloudiness is also increased over the Appalachian Mountains that are south-east of the Great Lakes.

Figure 1. Annual mean cloud amount from AVHRR PATMOS-x from 1982 to 2012. Mean constructed from NOAA-7, 9, 11, 12, 14–18 and METOP-02.
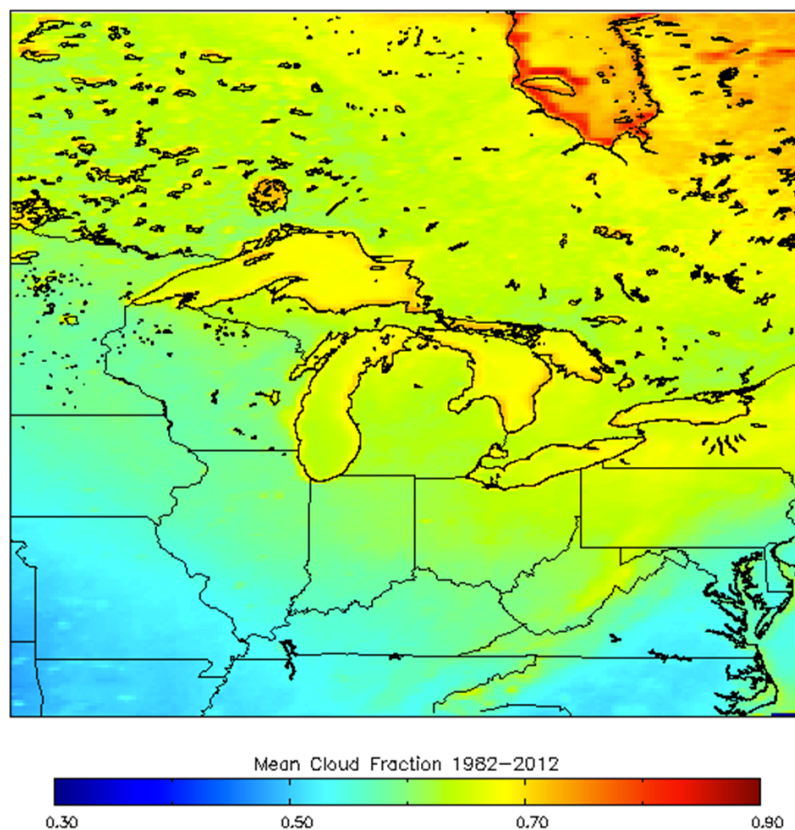
    Figure 2 is a time series of monthly mean cloud amount for the entire region over the time period. The grey area represents the uncertainty and the solid black line the mean. Daily mean values are calculated for each 1° × 1° box in the region, including a diurnal correction that addresses asymmetrical sampling of satellite equatorial crossing times due to satellite drift [4]. Monthly mean values are calculated from the daily means, while the uncertainty estimate is the standard deviation of daily values for each month; to which both natural variability and measurement uncertainty contribute. As with previous studies, [5–8] The figure depicts a strong seasonal cycle with maximum cloud amounts in the winter and minimum in summer, with an annual range in the cloud cover of ~20% to 30%. Cloud frequency is most affected during winter due to the large heat and moisture fluxes from the water to the air above [8]. A linear trend analysis indicates decreasing cloud cover of approximately 1% per decade for the entire region.

> **Figure 2.** The diurnally corrected time series of the monthly mean cloud cover over the Great Lakes region between 1982 and 2012. The geographic region is bounded by 55°N and 35°N latitude and between −75° and −95° longitude. The thin black line is the mean and the gray shade the uncertainty. Uncertainty was calculated as the standard deviation of daily values for each month.
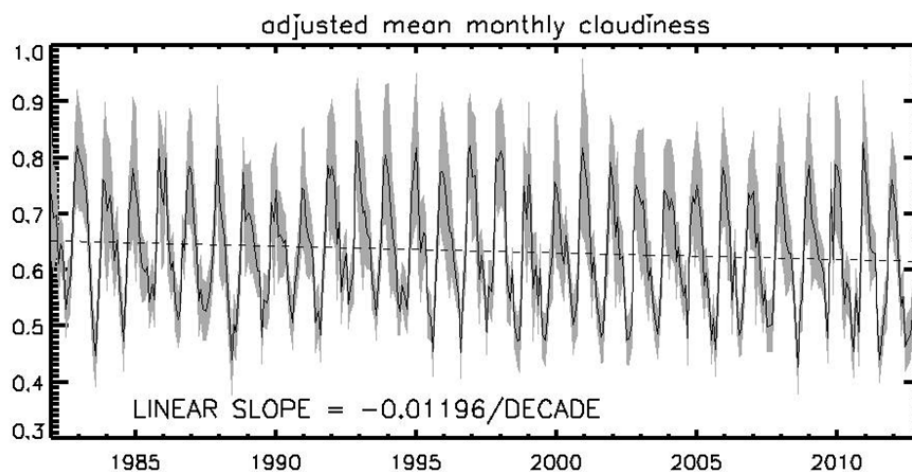

    Figure 3 depicts the PATMOS-x AVHRR annual linear trend maps over Great Lakes region with diurnal correction applied. The statistical approach used for this analysis comes from previous studies [9,10]. The uncertainty estimate used when calculating the linear slope of the record is the standard deviation of daily values for each month; to which both natural variability and measurement uncertainty contribute. For the slope of the linear fit, ω, we assume that a trend at the 95% confidence level is established when $|\omega/\sigma_\omega| > 2$, where σ_ω is the standard deviation of ω. Subsequently the number of years (n*) that it would take for ω to be considered a significant trend with a probability of 0.90 is:

$$n^* \approx \left[\frac{3.3\sigma_\varepsilon}{|\omega|(1-\phi)} \right]^{\frac{2}{3}} = \left[\frac{3.3\sigma_N}{|\omega|} \sqrt{\frac{1+\phi}{1-\phi}} \right]^{\frac{2}{3}} \quad (1)$$

where N is the noise of the time-series, ϕ is the autocorrelation of N, and ε is the white noise. This analysis is completed for each 1° × 1° box in the domain, resulting in estimates of ω and n*. Those

boxes for which the length of the record exceeds the n* estimate are overlaid by white stippling in Figure 3. There are significant decreasing trend in cloud amount over the Great Lakes of about −2% per decade. A decreasing trend in cloud amount is observed in each season over each of the Great Lakes, with slightly larger decreasing trends in autumn and summer seasons (Table 1).

Figure 3. The trends in cloud cover change over the region during the period 1982 and 2002. The white stippled areas indicate regions where the trend is significant according the [9,10] statistical test.
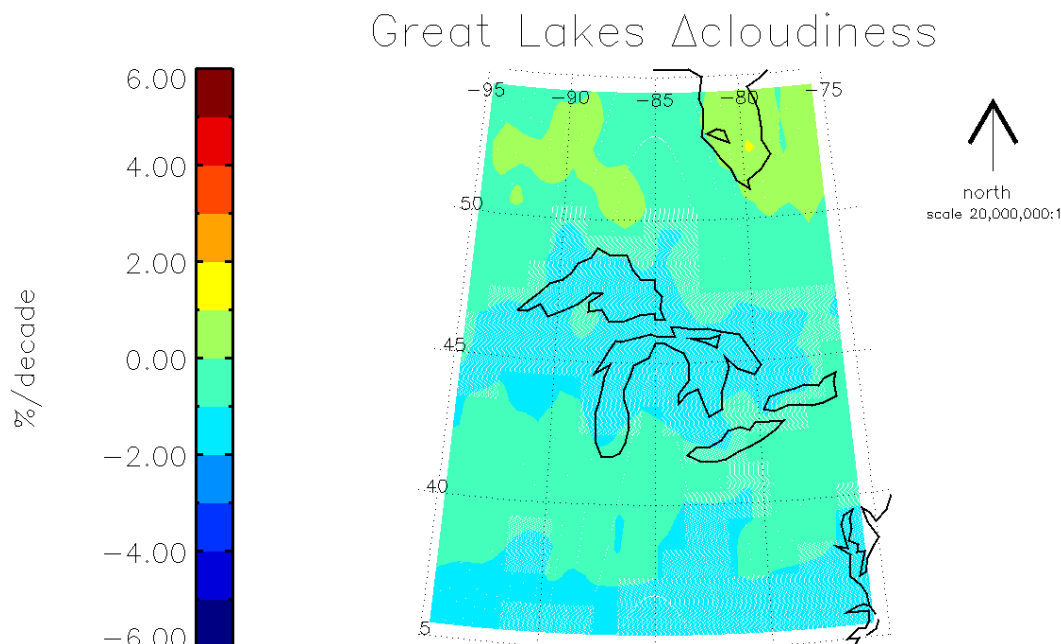

Table 1. Change in total cloudiness over land and water as measured from 1981 to 2012 using the PATMOS-x AVHRR record over the region show in Figure 3. The units are change in percent cloudiness per decade.

	Winter	Spring	Summer	Fall
Land	0.05	−1.09	−1.01	−2.30
Water	−0.81	−1.08	−1.82	−2.45

Figure 4 shows a box plot of cloud amount over the region as a function of month for land and water regions separately. As the satellites carrying the AVHRR precess with time, the four plots show the seasonal cycle during four local time periods (e.g., 0–6 local time, 6–12 local, 12–18 local and 18–24 local time). During winter, the cloud cover over the surface of the Great Lakes is greater than the cloud cover over land. The interquartile range is smaller during winter over the water, while smaller in the summer over land. During summer, the differences in cloud amount are smaller, and summer cloudiness over land is slightly larger than that over water. Shallow convection is less likely over the lakes between late spring and early autumn when the water bodies are cool compared to the land surface, which warms up rapidly. During winter, cloud is more common over the water than land. The Great Lakes are very cloudy during winter, more than 70% on average. This arises because the

frequency of fronts and cyclones in winter is high as the jet stream is further south than summer. Also, the lakes are often not completely ice covered (except perhaps Lake Erie) and so heat and moisture is added to the atmosphere in winter increasing cloudiness over the open waters.

Figure 4. Box plot of the monthly mean cloud cover over the Great Lakes and surrounding land. The four plots represent four local time periods as denoted in the legend.
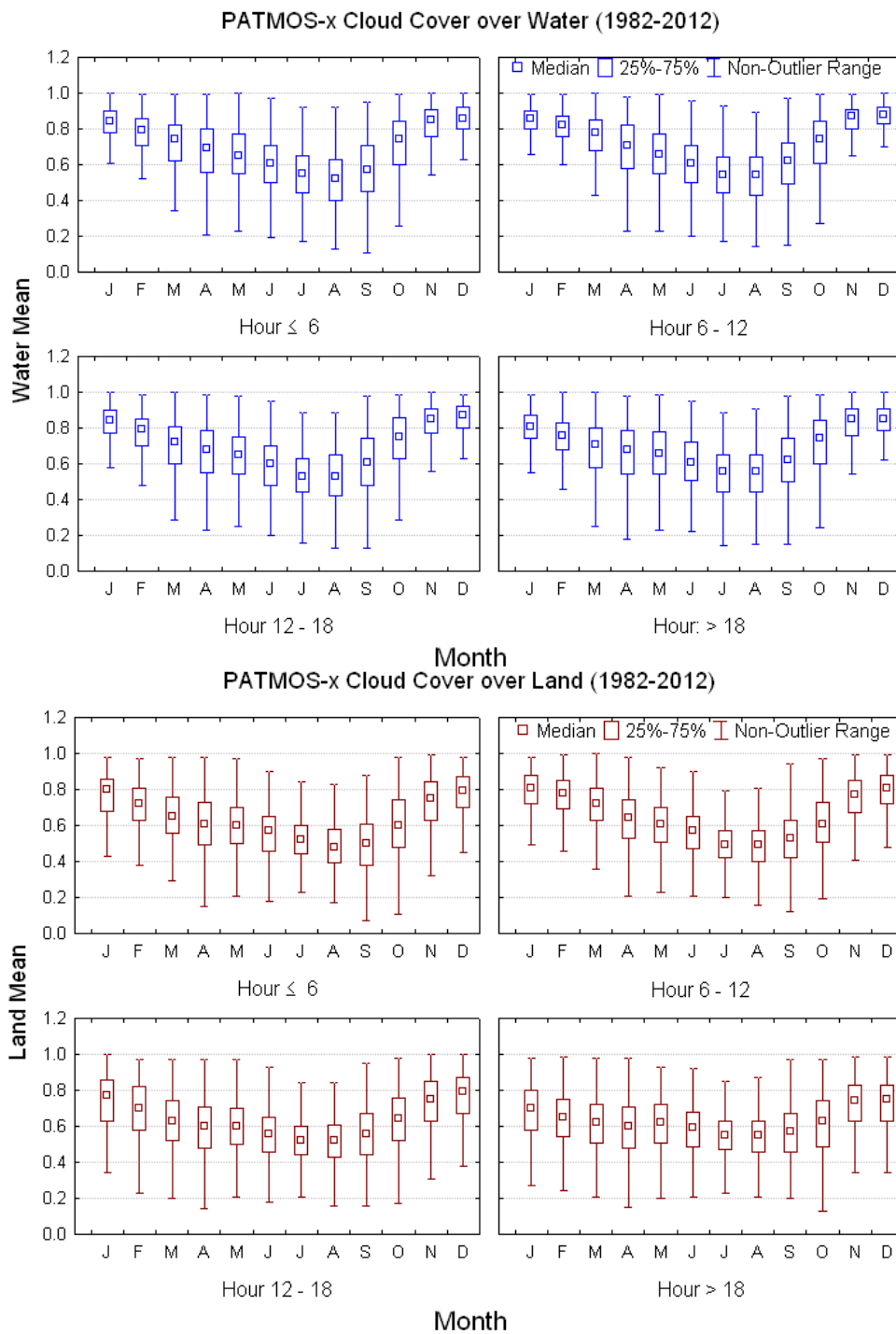
There is also strong seasonal variation in cloud amount over each lake (Figure 5). The annual cycle is similar for each lake, with maximum cloud cover in winter and minimum in summer. During winter moisture and sensible heat fluxes into cold air above creates instability that increases cloudiness and precipitation downwind [5,11]. Lake Superior and Lake Huron, the two most northern lakes, have greater cloud amounts in winter than the other lakes; consistent with the five winter periods studied by [11]. Figure 6 depicts the mean cloud cover for each lake as a function of Julian Day and the standard deviation in the 31-year record. The daily mean cloud amount over each lake in winter is generally greater than 80%. The minimum daily cloud amounts occur in late August, when cyclonic activity is a minimum over the Great Lakes [5]. The range in cloud amount between late summer and winter is approximately 40% to 50%. Figure 6b shows the standard deviation of the daily mean cloud cover for each lake as a function of Julian Day. The standard deviation is smallest in winter, as the cloud cover is generally high. Cloud variability is greatest in summer.

Figure 5. The mean cloud cover as a function of month for each of the Great Lakes. The point represents the mean and the whiskers the 95% confidence interval of the location of the mean.
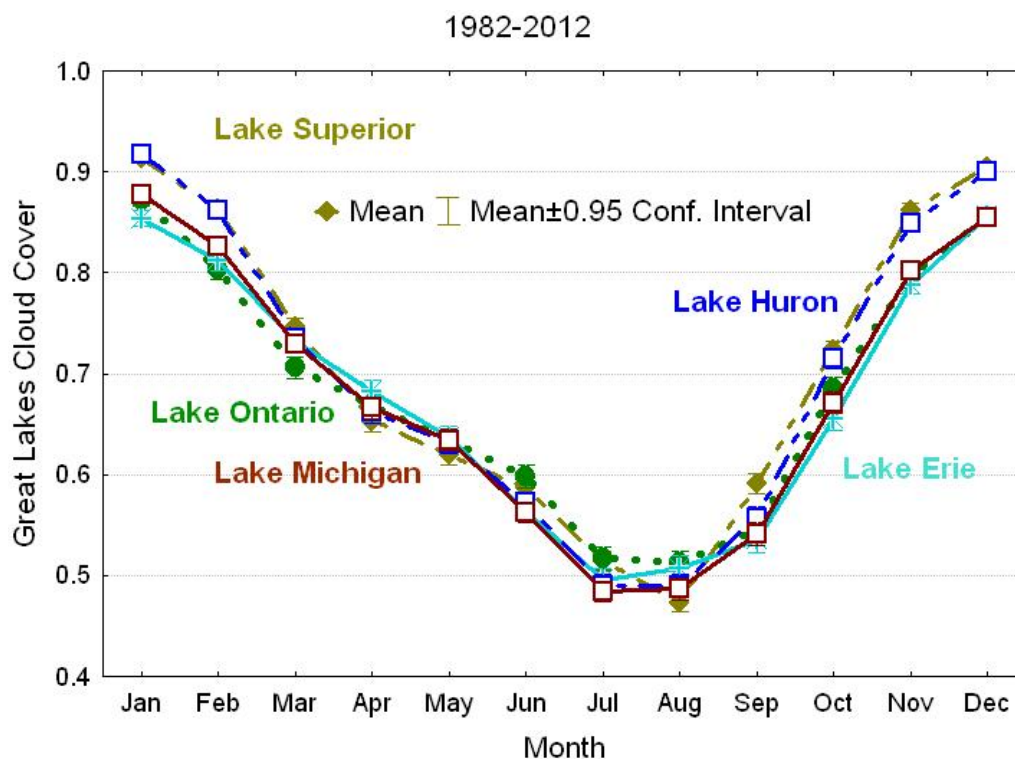

The resultant weather features, and thus climate, due to air mass modification by the Great Lakes are referred to as lake effects. Lake effect snow storms are well known, a result of air mass modification by the underlying relatively warm waters. To explore lake effect cloudiness, cloud amount was determined for the period and composited with respect to wind direction. The wind direction is taken from the Climate Forecast System Reanalysis (CFSR) data set as the mean direction at a height of 10 m above the area covered by the Great Lakes water region. The results of the composites are shown for each season in Figures 7–10 (summer, autumn, winter and spring). The wind

direction is shown in the lower left hand of each panel; the first panel is the seasonal mean of all wind directions. The frequency of each wind direction during the 31-year period is listed in the top of the panel.

Figure 6. (**a**) The 31-year average cloud amount over each Great Lake as indicated in the legend as a function of Julian Day. (**b**) The standard deviation of the daily cloud cover for each lake as indicated in the legend.
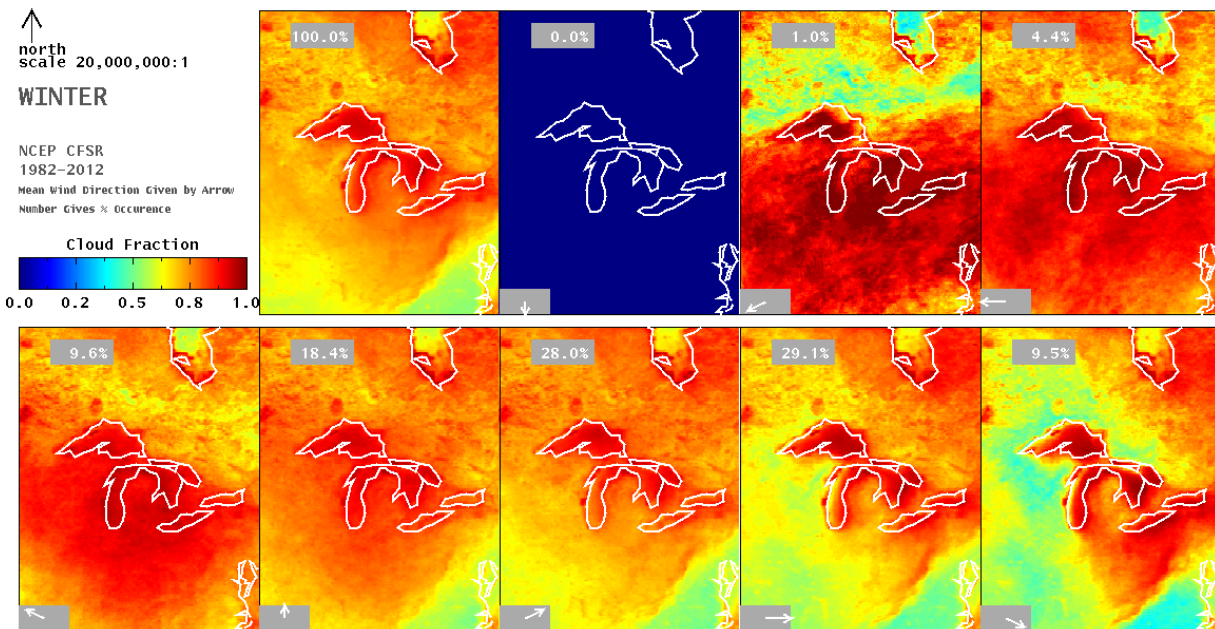

(**a**)

(**b**)
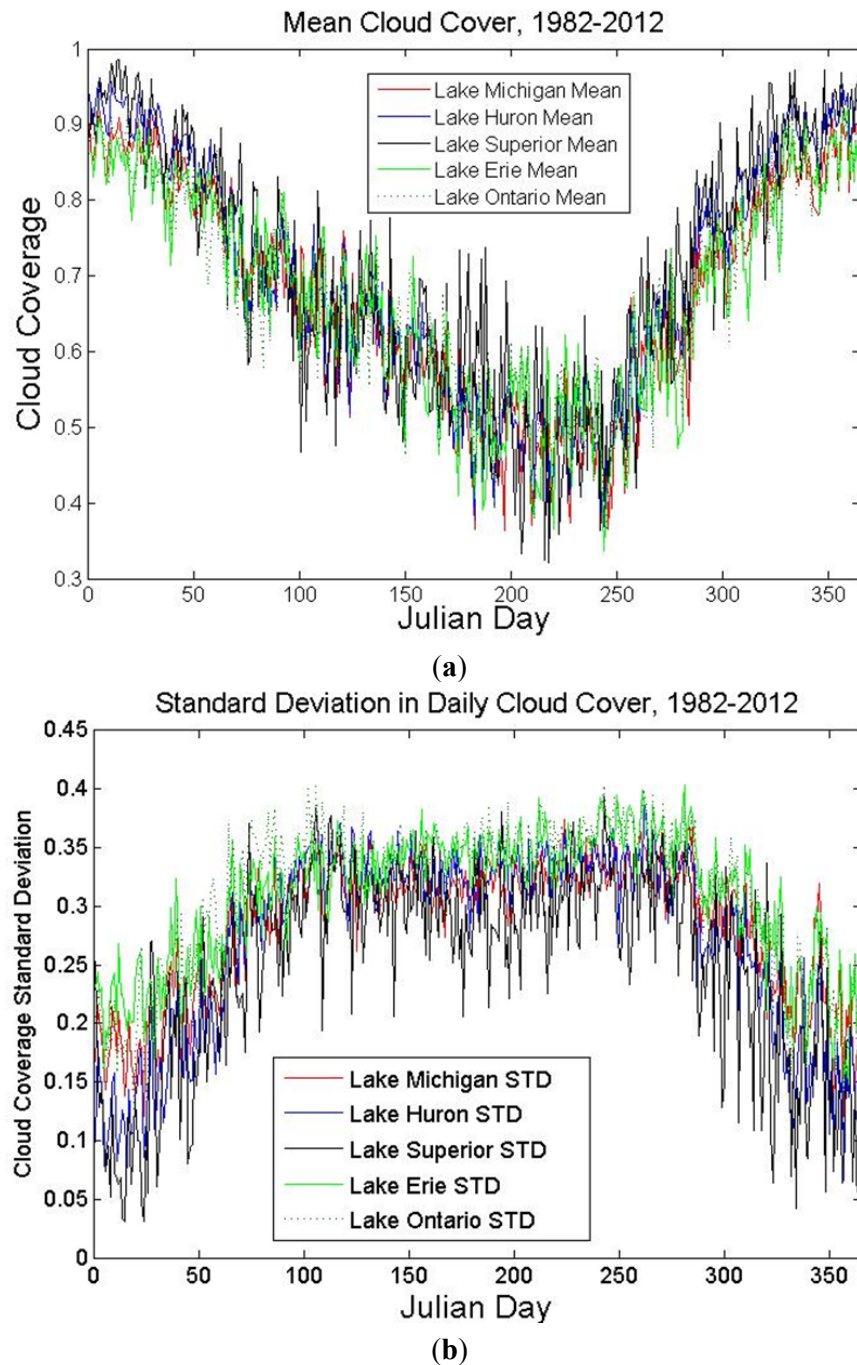
Figure 7. PATMOS-x cloud cover for the region during the 31-year time period during the summer months (June, July and August) composited with respect to wind direction. The wind direction is computed as the mean wind direction over a rectangle that covers all of the Great Lakes. The first panel represents the average summer cloud cover. The next panels represent the average cloud amount given the specified wind direction. The percentages of occurrences for a given wind condition are listed in the panel. There must be at least 10 occurrences to be compiled, so there are no northerly wind directions.
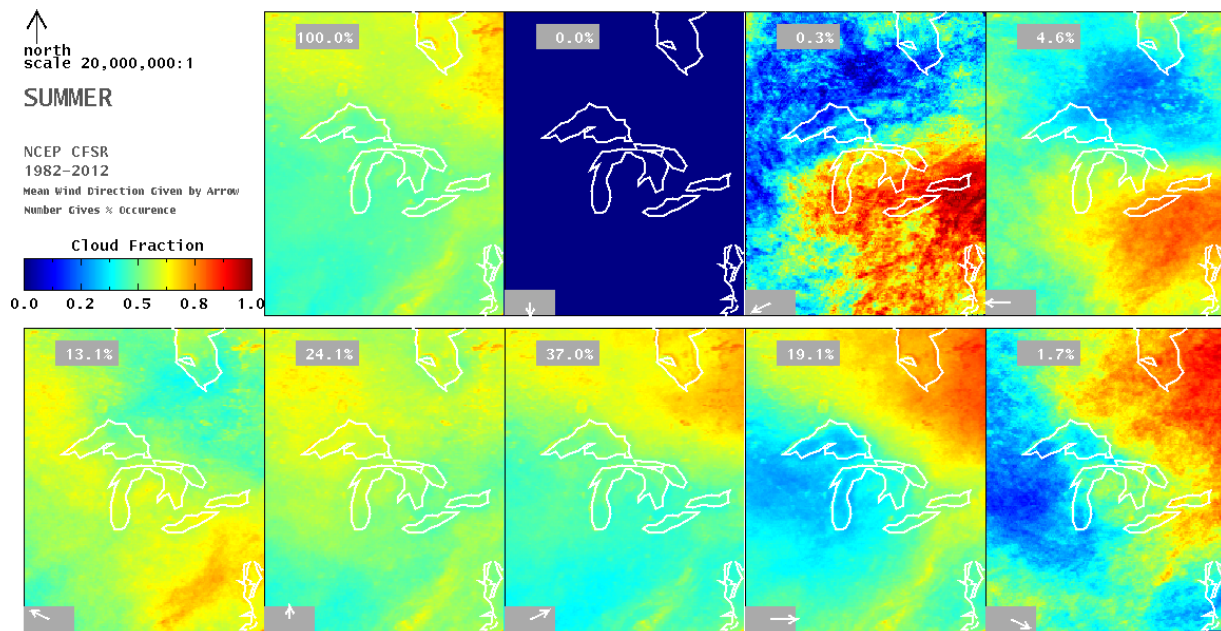

Figure 8. PATMOS-x cloud cover for the region during the 31-year time period during the autumn months (September, October, and November) composited with respect to wind direction. Same as Figure 7 except for autumn.
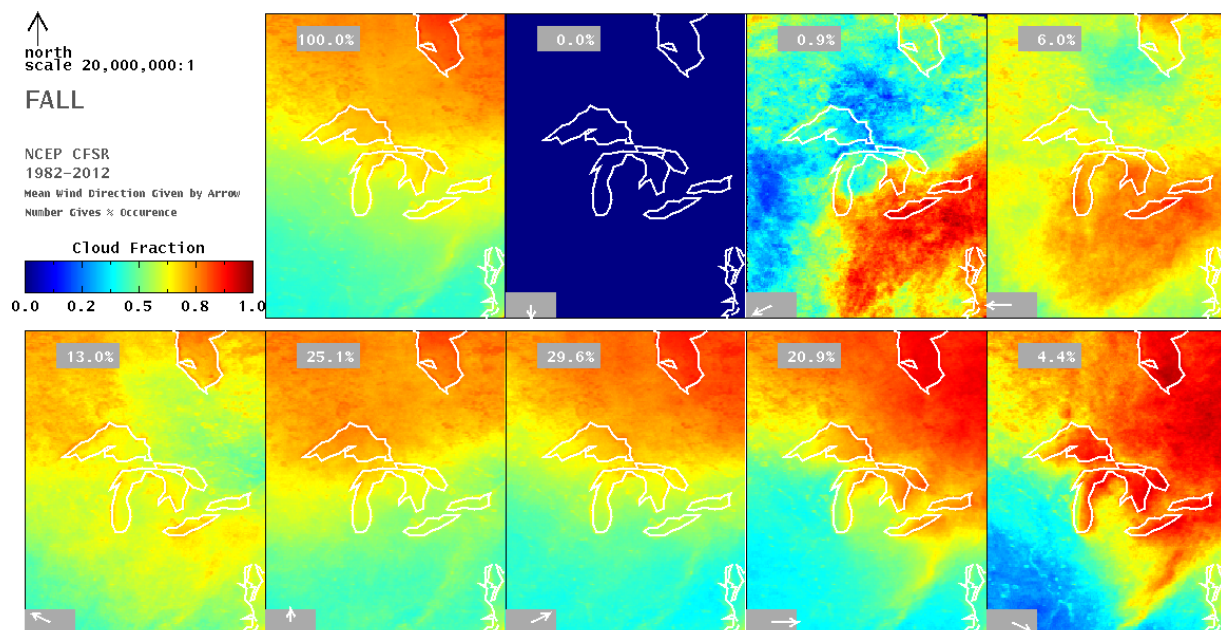
Figure 9. PATMOS-x cloud cover for the region during the 31-year time period during the winter months (December, January and February) composited with respect to wind direction. Same as Figure 7 except for winter.

Figure 10. PATMOS-x cloud cover for the region during the 31-year time period during the spring months (March, April and May) composited with respect to wind direction. Same as Figure 7 except for spring.
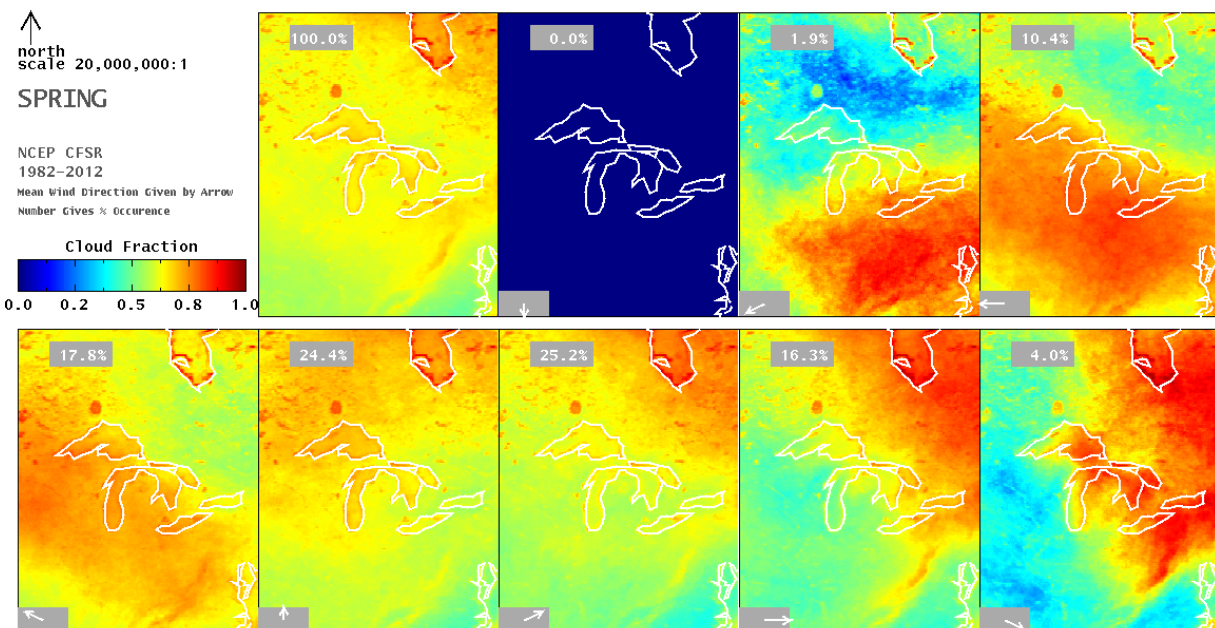
In the summer winds are primarily from the south-east to west directions. During summer, the lake surface temperatures are cooler than those of the surrounding land surface. During this season (Figure 7), in comparison to land, the lakes act to suppress certain cloud types such as shallow convection. The

cloud cover for the region typically ranges between 40% and 70%. Cloud cover of Lakes Superior and Michigan is small for winds from the west than for a southerly wind. The downwind impacts of the lake are not as strongly indicated in the cloud cover during summer as in the other seasons because of daytime mixing of the boundary layer due to daytime surface heating. Southerly and south-easterly winds bring moist low level air to the region, and cloud cover over the land to the south of the lakes is similar to that over the lakes. Westerly winds bring drier air and there is more contrast between the lakes and the adjacent land to the west and south. Autumn (Figure 8) season has more cloud over the lakes than summer; autumn also has a high fraction of cases with the wind from the south to west directions. The increased cloudiness downwind of the lakes is more evident in autumn than in summer. In early autumn, the water temperature becomes warmer than the land and remains so until early spring. This makes the lower boundary layer more unstable as air masses are modified as they pass over the lake, supporting the development of low level cloud.

In winter (Figure 9) the water surfaces are generally warmer than the adjacent land [5,6]. The greatest cloud amount for the lakes occurs during the winter time period. The impact of the open waters in increasing cloud cover is clearly seen in the mean map. Cloud cover increases to over 80% above the lakes, while over land the cloud cover amounts generally range between 30% to 60%. Upwind of the Great Lakes (e.g., Wisconsin and Canada) often have winter cloud cover ranging less than 30% while Michigan has a winter cloud cover of greater than 50%.

The flat lands to the north provide an easy exchange of cold Arctic air as it flows south. Anticyclones slip southward from the cold northern regions. As a result, there is a lake effect on cloud cover that is apparent in the wind direction composites. The Great Lakes modify the continental polar air masses [12–14] and, as a result, the northwesterly wind composite shows the western half of Lake Michigan and the north-western region of Lake Superior to have a much lower cloud amount that of the eastern portion of those lakes. This wind direction is associated with the cold air mass behind the passage of a cold front.

The low-pressure areas in spring may be frequent and perhaps more common over the more northern lakes; however the average spring time cloudiness is similar among the lakes. In early spring the cloud cover is about 75% and decreases to 65% in late spring (see Figure 5). Ice on the lakes can falsely be classified as cloud because of the decrease in contrast with cloud at infrared and visible wavelengths. The warmer land has a stronger infrared and visible contrast with a cloud over an ice covered lake, increasing the detectability of cloud than when cloud is over the cooler lake. For example, Lake Nipigon (north of Lake Superior) shows more cloud cover in the spring than the surrounding land surface; this is likely a result of ice on the lake being classified as cloud. Cloud detection difficulties can also occur along coastlines, where a pixel may be viewing some land but yet be classified as water. The brighter land surface may misguide solar and infrared channel spectral tests.

2.3. Wind Parallel Cloud Bands

During winter, the passage of cold air over the relatively warm waters of the Great Lakes results in the formation of a well-mixed convective layer with cumuliform cloud patterns. This condition is referred to as a Type I cloud topped boundary [13]. Analysis of GOES visible imagery from 5 winters [12] demonstrated that wind-parallel bands were common over the lakes in winter, particularly the western

lakes of Lake Superior, Lake Huron and Lake Michigan. Figure 11 is a satellite image of a polar air mass flowing over Lake Superior and Lake Michigan on 5 February 2007 generating wind parallel cloud bands. This example includes lake-to-lake cloud bands that extend from Lake Superior across to northern Lake Michigan. This condition of lake-to-lake cloud bands originating over Lake Superior occurred on 202 winter days during the 5-year period 2000–2004 [15].

> **Figure 11.** A polar air mass flowing over Lake Superior and Lake Michigan on 5 February
> 2007 generating wind parallel cloud bands over Lakes Superior and Michigan.
> The thin red line indicates the sampling region of the Cloud-Aerosol Lidar with Orthogonal
> Polarization (CALIOP.).
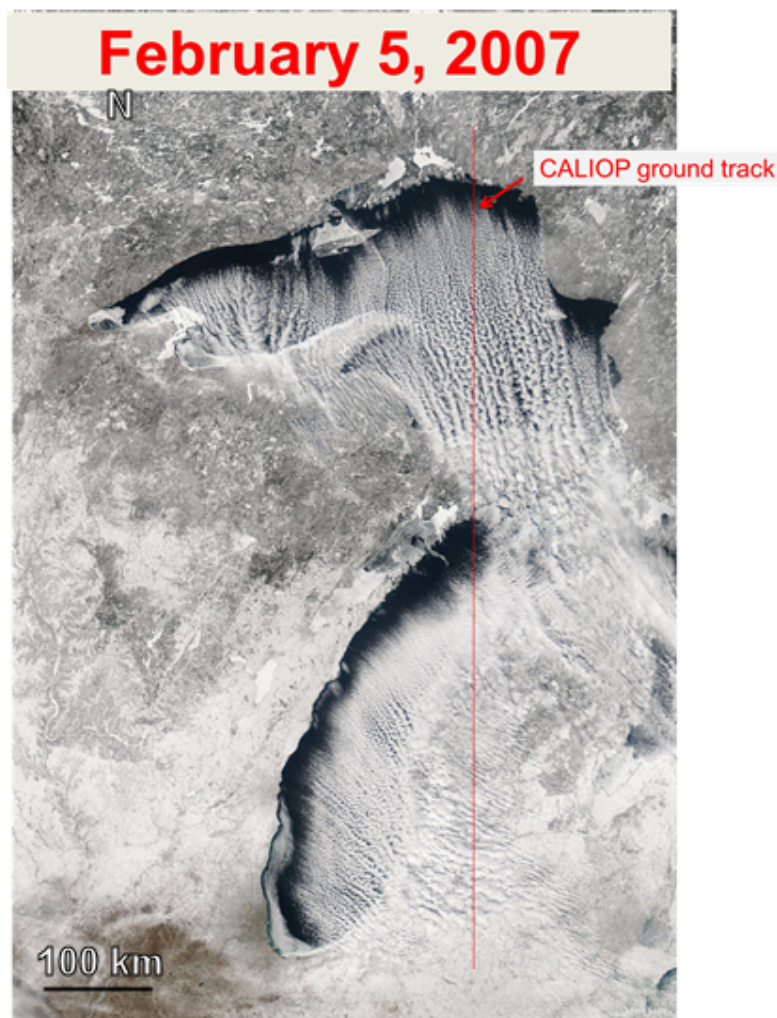
Monthly means can sometimes misrepresent the observations, or do not provide a complete picture of the dynamics related to the cloud formation. To explore these cloud properties, observations from the MODIS Aqua data are aggregated onto a 0.1 degree grid. The view angle of the observations included in the composite was limited to 35 degrees from nadir. The MODIS MYD35 and MYD06 Collection-5 cloud properties [16,17] are used in this study. Cloud properties are composited as a function of wind speed direction to explore how cloud top pressure, optical depth and particle size change downwind of the coastline and over the water. Those cloud properties were composited when

the wind direction at St. Paul, MN was from the Northwest for a two-day period. This occurred on 18 days in the winters of 2007 and 2008.

MODIS analysis of cloud cover (Figure 12) shows a similar distribution as that of AVHRR winter with northwest winds, with maximum cloud cover over the Great Lakes. During winter, cold air outbreaks over the Great Lakes generate low-level cloud amounts. The cloud frequency downwind of the coastline of Superior and Michigan approach 100%; near the upwind coast the frequency is less than 10%, in agreement previous observations [12,18–20]. The location of the cloud edge from the shore line ranges from approximately 10 to 50 km downwind and depends on the heat and moisture fluxes from the lake and the low-level static stability upwind of the lake [18].

Figure 12. Retrieved cloud properties from MODIS for cases of northwest winds over Lake Superior in winters of 2007 and 2008: (**a**) mean cloud amount; (**b**) mean cloud top pressure in mb; (**c**) mean optical depth for ice cloud; (**d**) effective radius for ice particles in microns and (**e**) mean effective radius of water drops in microns. Land regions are masked as green.
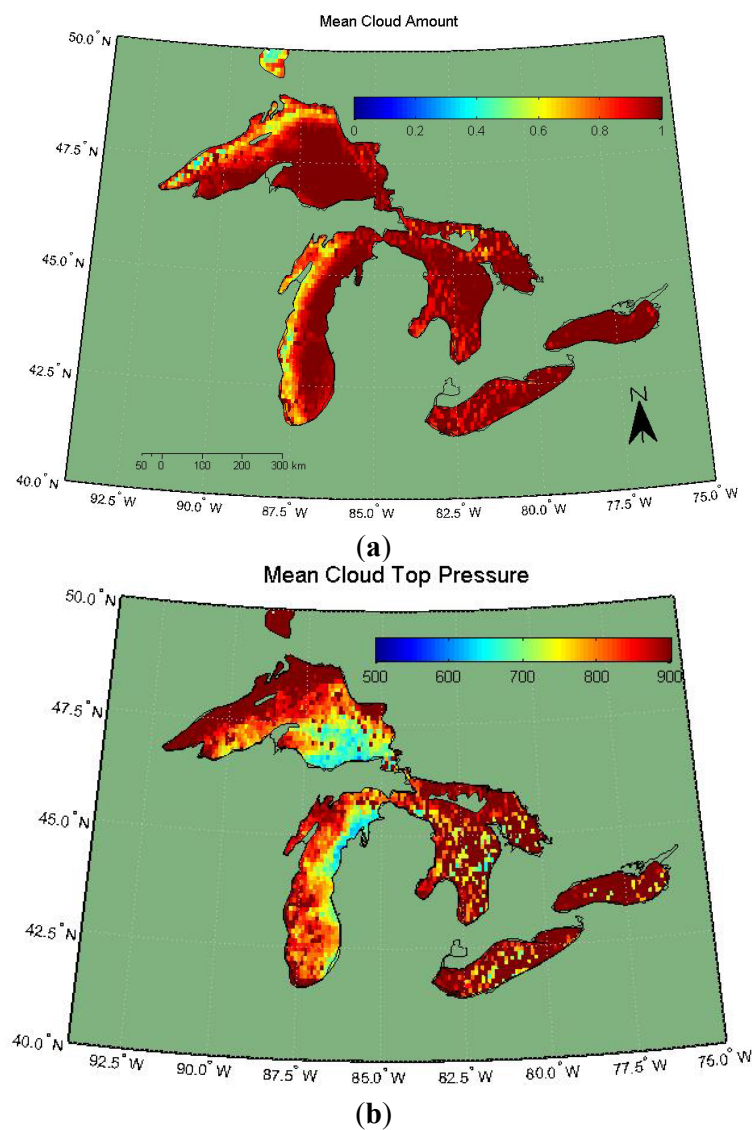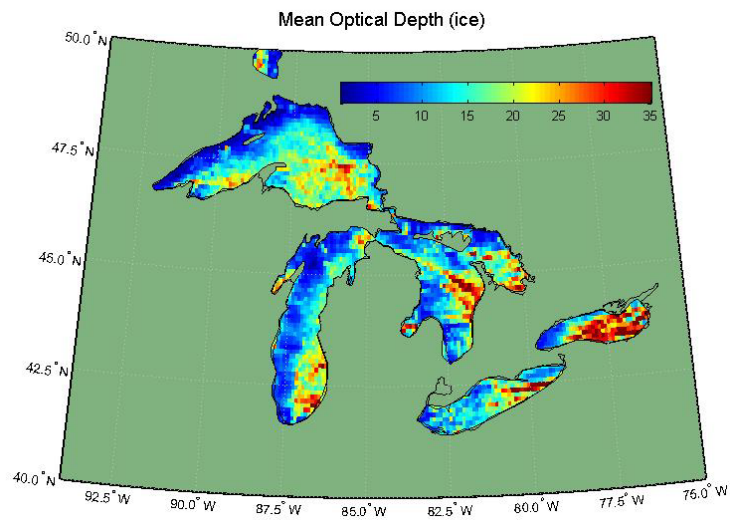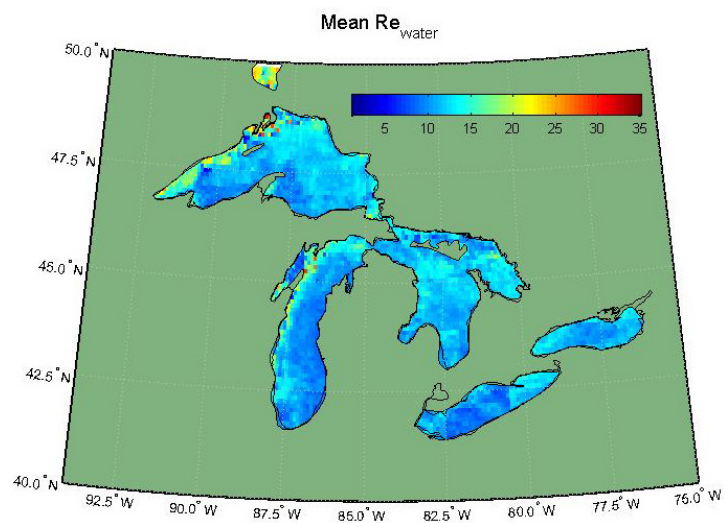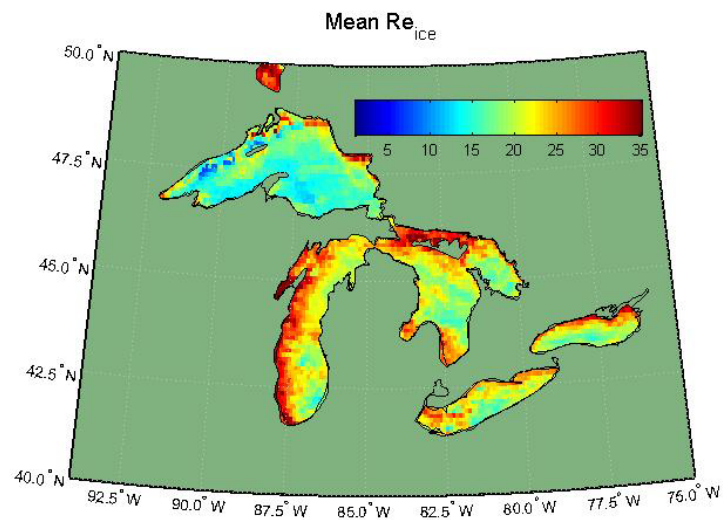

(**a**)


(**b**)

Figure 12. *Cont.*

(c)

(d)

(e)

Increases in cloud feature sizes are generally associated with increases in the depth of the convective boundary layer [20] and as the vertical extent of the cloud field develops, the cloud top pressure decreases from approximately 900 mb to 650 mb downwind. These changes in cloud top altitude downwind of the coastline was observed using aircraft [20]. The satellite retrieval has a lower pressure than previous studies [20–22]. For low cloud cover associated with a surface temperature inversion, the MODIS retrievals tend toward a lower pressure than collocated lidar observations [23,24]. The authors of [21] observed that cloud is limited to the convective internal boundary layer, located in the transition zone above the mixed layer. The convective internal boundary layer grows downstream [25]. The increase in cloud altitude downwind of the shoreline is also observed in the lidar observations of the Cloud-Aerosol Lidar and Infrared Pathfinder Satellite Observations (CALIPSO) mission [26] (Figure 13). This increase in cloud top altitude is better aligned with the study of [20].

Figure 13. Lidar observations over Lake Superior on 5 February 2007 showing the increase of cloud top altitude downwind, wind direction is from right to left. The right red bar indicates the location of Lake Superior that the lidar sampled and the left most red line Lake Michigan overpass.
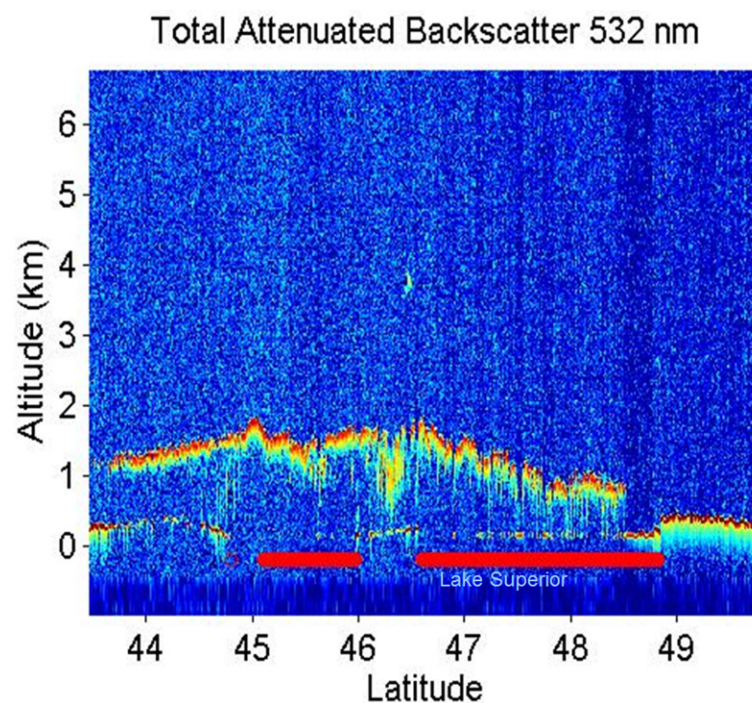
The optical depth also increases downwind over these lakes [20] and this is captured in the MODIS retrieval composite. The MODIS cloud phase retrieval indicates water, ice and mixed phase cloud, in agreement with observations [27]. For water cloud, the retrieved effective radius of the cloud remains fairly constant between about 10 and 15 µm downwind of the coastline. The retrieved effective radius for ice cloud shows generally larger particles than for the water cloud.

3. Conclusions

This paper provides a regional climatology of cloud cover over the Great Lakes region, derived from 31-years of satellite observations. The analysis of the 31-year AVHRR data set is consistent with previous studies of the Great Lake cloud cover:

- The lakes and the land have a strong seasonal variation with a range in cloudiness from less than 50% in summer to over 80% percent in winter.
- During winter the Great Lakes are cloudier than the surrounding land.
- Lake Superior and Huron have the greatest cloud amounts in winter.
- There is a slight decreasing trend in cloud cover for the region during the time period. The trend is greatest, and significant, over the water bodies.
- Cloud amount composited with wind direction demonstrates that the increasing cloud amounts downwind of the lakes are greatest during the autumn and winter.

This paper also investigates the properties of parallel wind cloud bands by compositing retrieved cloud properties from the MODIS instrument. As expected, cloud increased in vertical extent downwind from the coast. The optical depth of the cloud also increases. The retrieved ice effective radii increases then decreases to a nominal value of approximately 15 to 18 μm downwind of the coastline. The retrieved effective radii of water phase cloud are slightly smaller.

Conflicts of Interest

The authors declare no conflict of interest.

References

1. Heidinger, A.K.; Foster, M.J.; Walther, A. The pathfinder atmospheres extended (PATMOS-x) AVHRR climate data set. *Bull. Am. Meteor. Soc.* **2013**, doi: 10.1175/BAMS-D-12-00246.1.
2. Saha, S.; Moorthi, S.; Pan, H.-L.; Wu, X.; Wang, J.; Nadiga, S.; Tripp, P; Kistler, R.; Woollen, J.; Behringer, D.; *et al.* The NCEP climate forecast system reanalysis. *Bull. Am. Meteor. Soc.* **2010**, *91*, 1015–1057.
3. Heidinger, A.K.; Evan, A.T.; Foster, M.J.; Walther, A. A naive Bayesian cloud detection scheme derived from CALIPSO and applied within PATMOS-x. *J. Appl. Meteor. Climatol.* **2012**, *51*, 1129–1144.
4. Foster, M.J.; Heidinger, A. PATMOS-x: Results from a diurnally corrected 30-yr satellite cloud climatology. *J. Clim.* **2013**, *26*, 414–425.
5. Eichenlaub, V.L. *Weather and Climate of the Great lakes Regions*; The University of Notre Dame Press: Notre Dame, IN, USA, 1979; p. 335.

6. Changnon, S.A.; Jones, D.M.A. Review of the influences of the Great Lakes on weather. *Water Resour. Res*. **1971**, *8*, 360–371.

7. Bates, G.T.; Hostetler, S.W.; Giorgi, F. Two-year simulation of the Great Lakes region with a coupled modeling system. *Mon. Wea. Rev.* **1995**, *123*, 1505–1553.

8. Scott, R.W.; Huff, F.A. Impacts of the Great Lakes on regional climate conditions. *J. Great Lake. Res*. **1996**, *22*, 845–863.

9. Weatherhead, E.C.; Reinsel, G.C.; Tiao, G.C.; Meng, X.-L.; Choi, D.; Cheang, W.-K.; Keller, T.; DeLuisi, J.; Wuebbles, D.J.; Kerr, J.B.; *et al.* Factors affecting the detection of trends: Statistical considerations and applications to environmental data. *J. Geophys. Res*. **1998**, *103*, 17,149–161.

10. Weatherhead, E.C.; Stevermer, A.J.; Schwartz, B.E. Detecting environmental changes and trends. *Phys. Chem. Earth* **2002**, *27*, 399–403.

11. Kristovich, D.A.; Steve, R.A., III. A satellite study of cloud-band frequencies over the Great Lakes. *J. Appl. Meteorol.* **1995**, *34*, 2083–2090.

12. Lenschow, D.H. Two examples of planetary boundary layer modification over the Great Lakes. *J. Atmos. Sci.* **1973**, *30*, 568–581.

13. Agee, E.M. Mesoscale cellular convection over the oceans. *Dyn. Atmos. Ocean*. **1987**, *10*, 317–341.

14. Braham, R.R., Jr.; Kelly R.D. Lake-Effect Snow Storms on Lake Michigan, USA. In *Cloud Dynamics*; Agee, E., Asai, T., Reidel, D., Eds.; D. Reidel Publishing Company: Dordrecht, The Netherlands, 1982; pp. 87–101.

15. Rodrigues, Y.; Kristovich, D.A.R.; Hjelmfelt, M.R. Lake-to-lake cloud bands: Frequencies and locations. *Mon. Wea. Rev.* **2007**, *135*, 4202–4213.

16. Ackerman, S.A.; Holz, R.E.; Frey, R.; Eloranta, E.W.; Maddux, B.; McGill, M. Cloud detection with MODIS: Part II. Validation. *J. Atmos. Ocean. Technol.* **2008**, *25*, 1073–1086

17. Platnick, S.; King, M.D.; Ackerman, S.A.; Menzel, W.P.; Baum, B.A.; Riédi, J.C.; Frey, R.A. The MODIS cloud products: Algorithms and examples from Terra. *IEEE Trans. Geosci. Remote Sens*. **2003**, *41*, 459–473.

18. Kristovich, D.A.R.; Laird, N.F. Observations of widespread lake-effect cloudiness: Influences of lake surface temperature and upwind conditions. *Weather Forecast.* **1998**, *13*, 811–821.

19. Kristovich, D.A.R. Mean circulations of boundary-layer rolls in lake-effect snow storms. *Bound.-Layer Meteorol.* **1993**, *63*, 293–315.

20. Chang, S.S.; Braham, R.R. Observational study of a convective internal boundary layer over Lake Michigan. *J. Atmos. Sci.* **1991**, *48*, 2265–2279.

21. Agee, E.M.; Gilbert, S.R. An aircraft investigation of mesoscale convection over Lake Michigan during the 10 January 1984 cold air outbreak. *J. Atmos. Sci.* **1989**, *46*, 1877–1897.

22. Kristovich, D.A.R.; Laird, N.F.; Hjelmfelt, M.R. Convective evolution across Lake Michigan during a widespread lake-effect snow event. *Mon. Wea. Rev.* **2003**, *131*, 643–655.

23. Baum, B.A.; Menzel, W.P.; Frey, R.A.; Tobin, D.C.; Holz, R.E.; Ackerman, S.A.; Heidinger, A.K.; Yang, P. MODIS cloud top property refinements for Collection 6. *J. Appl. Meteorol. Climatol*. **2012**, *51*, 1145–1163

24. Holz, R.E.; Ackerman, S.A.; Nagle, F.W.; Frey, R.; Kuehn, R.E.; Dutcher, S.; Vaughan, M.A.; Baum, B. Global MODIS cloud detection and height evaluation using CALIOP. *J. Geophys. Res.* **2008**, *113*, D00A19-1–D00 A19-17.

25. Stunder, M.; SethuRaman, S. A comparative evaluation of the coastal internal boundary-layer height equations. *Bound.-Layer Meteorol.* **1985**, *32*, 177–204.

26. Winker, D.M.; Pelon, J.; Coakley, J.A., Jr.; Ackerman, S.A.; Charlson, R.J.; Colarco, P.R.; Flamant, P.; Fu, Q.; Hoff, R.; Kittaka, C.; *et al.* The CALIPSO Mission: A global 3D view of aerosols and clouds. *Bull. Am. Meteor. Soc.* **2010**, *91*, 1211–1229.

27. Kristovich, D.A.R.; Young, G.S.; Verlinde, J.; Sousounis, P.J.; Mourad, P.; Lenschow, D.; Rauber, R.M.; Ramamurthy, M.K.; Jewett, B.F.; Beard, K.; *et al.* The lake-induced convection experiment and the snowband dynamics project. *Bull. Am. Meteor. Soc.* **2000**, *81*, 519–542.